ScientificScholar®
Knowledge is power
Publisher of Scientific Journals

www.surgicalneurologyint.com

Surgical Neurology International

Editor-in-Chief: Nancy E. Epstein, MD, Professor of Clinical Neurosurgery, School of Medicine, State U. of NY at Stony Brook.

SNI: Neurovascular

Editor
Kazuhiro Hongo, MD
Shinshu University, Matsumoto, Japan

SNI
Open Access

Original Article

Exploring the hemodynamic behavior of residual aneurysms after coiling and clipping: A computational flow dynamic analysis

Christopher S. Ogilvy[1], Rafael Trindade Tatit[2], Vincenzo T. R. Loly[2], Felipe Ramirez-Velandia[1], João S. B. Lima[3], Carlos E. Baccin[4]

[1]Division of Neurosurgery, Beth Israel Deaconess Medical Center, Harvard Medical School, Boston, United States, [2]Instituto Israelita de Ensino e Pesquisa, Hospital Israelita Albert Einstein, [3]Mechanical Engineering Department, Maua Institute of Technology, [4]Interventional Neuroradiology, Hospital Israelita Albert Einstein, São Paulo, Brazil.

E-mail: Christopher S. Ogilvy - cogilvy@bidmc.harvard.edu; *Rafael Trindade Tatit - rtrindadetatit@gmail.com; Vincenzo T. R. Loly - vincenzololy@hotmail.com; Felipe Ramirez-Velandia - felipegolframirez@gmail.com; João S. B. Lima - joao.brasil@maua.br; Carlos E. Baccin - carlos.baccin@einstein.br

***Corresponding author:**
Rafael Trindade Tatit, Instituto Israelita de Ensino e Pesquisa, Hospital Israelita Albert Einstein, São Paulo, Brazil.

rtrindadetatit@gmail.com

Received: 14 August 2024
Accepted: 18 September 2024
Published: 18 October 2024

DOI
10.25259/SNI_686_2024

Quick Response Code:

ABSTRACT

Background: Residual intracranial aneurysms post-clipping or coiling pose a poorly established risk of rupture. Computational fluid dynamic (CFD) offers insights into hemodynamic changes following such interventions. This study aims to assess hemodynamic parameters in residual aneurysms pre- and post-treatment with surgical clips or coils using CFD.

Methods: A retrospective analysis of consecutive patients between January 2015 and January 2024 was conducted. Digital subtraction angiography images were reconstructed using 3D modeling techniques, and hemodynamic parameters were analyzed with ANSYS® software.

Results: Six aneurysms were analyzed: Five unruptured and one ruptured. The aneurysms were located at the basilar apex (2), middle cerebral artery bifurcation (2), and origin of the posterior communicating artery (2). Post-treatment, there was a significant reduction in both aneurysm area (median reduction of 33.73%) and volume (median reduction of 25.3%). Five of the six cases demonstrated fewer low wall shear stress (WSS) areas, which could indicate a reduction in regions prone to thrombus formation and diminished risk of rupture. In the unruptured aneurysms, there was a median increase of 137.6% in average WSS. Notably, the only case with increased low WSS area also had the highest increase in average WSS. One basilar artery aneurysm showed increased WSS across all parameters, suggesting a higher rupture risk.

Conclusion: The increase in average and high WSS area, along with a decrease in low WSS area, reflects a complex balance between factors of stability and rupture risk. However, a simultaneous increase in all WSS parameters may represent the highest rupture risk due to increased mechanical stress on the aneurysm wall, necessitating closer monitoring.

Keywords: Computational fluid dynamics, Low shear area, Residual intracranial aneurysms, Wall shear stress

INTRODUCTION

Background

Intracranial residual intracranial aneurysms (IAs) are those with angiographic evidence of persistent filling after treatment. The frequency of incomplete aneurysm occlusion after surgical clipping varies from 4.7% to 23%[1,11,14] and after endovascular coiling from 9.5% to 46%.[3,10,19] Previous works have demonstrated that residual IAs after clipping harbor a significantly higher rupture risk than that of unruptured or *de novo* IAs [16,18,20] and the degree of aneurysm occlusion after initial treatment, whether surgical clipping or coiling, appears to be a strong predictor of the risk of subsequent rupture in patients presenting with subarachnoid hemorrhage.[7]

Given the elevated prevalence of residual aneurysms and the potentially heightened risk of rupture in these instances, there is a considerable need for the development of tools and the establishment of adjunct parameters in stratifying the risk of these residual aneurysms. In this context, computational fluid dynamics (CFD) appears to offer insights into hemodynamic factors that may influence the rupture of these aneurysms. A meta-analysis suggested that decreased local wall shear stress (WSS) may be an important predictive parameter of aneurysm rupture.[22] Another study indicated that ruptured aneurysms were more likely to have a greater low WSS area ratio and that aneurysm morphology could affect the distribution and magnitude of WSS, with both high and low WSS contributing to focal wall damage and rupture.[12] Furthermore, ruptured aneurysms have been shown to have a greater portion under low WSS, and low WSS was significantly associated with a higher risk of IA rupture as determined by the PHASES score.[8,17] In this context, analyzing residual aneurysms with CFD can provide valuable insights into the rupture risk of these aneurysms and assist in planning and making therapeutic decisions for these common findings.

Objectives

Herein, we assess hemodynamic parameters before and after treatment with surgical clips or coils on residual IAs using CFD. Insights into the most affected parameters by the respective treatments will be derived.

MATERIALS AND METHODS

This study was reviewed and approved by the institutional ethics committee. Informed consent was obtained from all patients or their next of kin.

Patient data

We conducted a retrospective investigation of data from consecutive patients treated between January 2015 and January 2024 for both ruptured and unruptured IAs, either by surgical clipping or coil embolization, with or without associated stenting. These patients exhibited residual aneurysms or necks on follow-up digital subtraction angiography (DSA). All digital angiography images of selected patients, both pre-and post-treatment, were anonymized.

Geometry reconstruction

For aneurysm geometry reconstruction, selected digital angiography examinations were processed using the 3D Slicer package, a software designed for 3D reconstruction and geometric analysis of vascular image-based modeling. From these images, stereolithography (STL) segmentations were created and subsequently imported into the SpaceClaim computer-aided design software for geometry processing. Following preparation, the mesh generation step was carried out using Ansys Fluent Meshing. Reconstructed geometries were compared with patient images and discussed with an interventional neuroradiologist for model approval.

Hemodynamic models

The numerical simulations were carried out in the software Fluent, part of the ANSYS® package. To handle fluid-structure interaction, we employed a partitioned coupling scheme specifically developed for incompressible flows interacting with solids subject to elastic or plastic deformations, as observed in arteries.

To estimate the average flow rate of each artery, we relied on the study by Zarrinkoob *et al*.,[21], which provided a detailed analysis of blood flow distribution in cerebral arteries using high-resolution phase-contrast magnetic resonance imaging. As for the normalized flow curve, we based our reference on the findings presented by Ford *et al*.[5]

Hemodynamic parameters

We analyzed the volume, surface area, and WSS before and after aneurysm treatment, as well as WSS in adjacent arteries. From flow velocity and pressure fields, we derived stress and strain fields of artery and aneurysm walls. These fields were used to calculate parameters such as WSS and their derivatives, as well as the magnitude of wall deformations caused by velocity and pressure fields. Similarly to the study by Hu *et al*.,[6] the low WSS area was defined as the areas of the aneurysm wall exposed to a WSS below 10% of the mean parent vessel WSS, then normalized by the dome area.

RESULTS

Aneurysm characteristics

Six patients with single cerebral aneurysms were included in this study, with pre-and post-treatment DSA images available

for analysis. Regarding the aneurysm locations, two were in the middle cerebral artery (MCA), two at the apex of the basilar artery, and two in the posterior communicating artery (PComA) with the internal carotid artery (ICA). Among these six identified aneurysms, five were treated with coil embolization and one with surgical clipping, situated in the MCA. Regarding rupture status, only one case was ruptured before treatment, located at the apex of the basilar artery.

Hemodynamic parameters in the pre-clipping and coil model

Two unruptured aneurysms at the bifurcation of the MCA were evaluated: one was treated with a surgical clip, and the other with endovascular coils and a Y-stent (Neuroform EZ). The surgical case aneurysm dome area was 60.65 mm^2, volume 48.78 mm^3, average WSS 14.28 Pa, and low WSS area 0.2%. The endovascular case aneurysm dome area was 215.88 mm^2, volume 289.85 mm^3, average WSS 2.44 Pa, and low WSS area 7.49%.

Two unruptured aneurysms at the bifurcation of the PComA with the ICA were treated with coils. One of the aneurysms had a dome area of 279.02 mm^2, a volume of 379.28 mm^3, an average WSS of 0.35 Pa, and a low WSS area of 74.9%. Another aneurysm had a dome area of 181.29 mm^2, volume of 208.73 mm^3, average WSS of 1.41 Pa, and low WSS area of 55.8%.

Two aneurysms at the apex of the basilar artery were treated endovascularly, one unruptured and another ruptured. The unruptured case was treated with coils and a stent (Neuroform Atlas) left under the P1 segment of the posterior cerebral artery (PCA). The aneurysm dome area was 207.47 mm^2, volume 306.97 mm^3, average WSS 2.41 Pa, and low WSS area 1.38%. The ruptured case was treated only with coils. The aneurysm dome area was 72.3 mm^2, volume 51.99 mm^3, average WSS 8.31 Pa, and low WSS area 21.7%.

Comparing pre- and post-clipping and coil model

After treatment, there was a reduction in both the area (median 33.74%; interquartile range [IQR] = 18.83%) and volume (median 19.37%; IQR = 23.43%) of all six identified aneurysms. Only one of the aneurysms was ruptured at the initial presentation. Among the cases analyzed, five exhibited increases in average WSS after treatment (median increase of 137.6%; IQR = 136.9%), five demonstrated a reduction in the low WSS area (median decrease of 70%; IQR = 49.72%), and five cases displayed an increase in high WSS area (median increase of 317.9%; IQR = 364.14%). When considering the location, it is notable that the two aneurysms located at the bifurcation of the MCA exhibited a reduction in the low WSS area (0.2–0.006% and 7.49–3.57%), coupled with an elevation in the average WSS (increase of 23.67% and 94.71%). Notably, among these, the residual aneurysm displayed a comparatively minor reduction in size, with its remaining portion constituting 58.61% of the original total volume, and also demonstrated a decrease in the high WSS area (99.1–94.6%). Regarding the two cases identified at the origin of the PComA, both demonstrated similar behavior of increased average WSS (an increase of 191.43% and 137.59%) and high WSS area (0.5–4.87% and 5.2–9.11%) and decreased low WSS area (74.9–66.7% and 55.8–4.98%). Finally, two cases at the basilar apex exhibited markedly different behaviors. Although both experienced an increase in the high WSS area (6.23–33.6% and 49.2–50.6%), the ruptured aneurysm demonstrated decreases in both average WSS (decrease 9.96%) and low WSS area (21.7–6.15%), whereas the unruptured case demonstrated increases in both average WSS (increase 200.83%) and low WSS area (1.38–7.82%). Notably, this unique case with an increase in low WSS area was the one with the highest increase in average WSS, both in relative (an increase of 200.83%) and absolute terms (an increase of 4.84 Pa). A detailed description of the hemodynamic parameters of each of the residual aneurysms and changes after treatment is shown in Tables 1 and 2.

Long-term outcomes of conservative and reintervention strategies

Both MCA residual aneurysms were managed conservatively, remaining without bleeding for 7 and 9 years up to the present date. On the other hand, both PComA-ICA residual aneurysms underwent successful reintervention with flow diverter stents, achieving complete occlusion until the last follow-up, 7 months after the reinterventions. Finally, the basilar artery apex residual aneurysm that had previously ruptured at the initial presentation remained stable without new hemorrhagic events for 3 years up to this moment. On the other hand, the other basilar artery apex residual aneurysm was retreated with the placement of another stent and coils, creating a Y-stenting, achieving complete occlusion until the last follow-up, 6 months post-reintervention.

Illustrative case (MCA)

A 62-year-old female experienced subarachnoid hemorrhage due to the rupture of an aneurysm in the ICA. The ruptured aneurysm was treated endovascularly with coils, achieving complete obliteration. Incidentally, another aneurysm was identified in the MCA, which was later treated surgically. However, post-surgical digital angiography revealed a residual portion of the clipped aneurysm. Following surgery, this residual aneurysm was evaluated using CFD, comparing its morphology and hemodynamics to its pre-treatment state [Figure 1].

The residual volume was calculated at 58.61% of the initial volume (48.78–28.59 mm^3), and although the average WSS

Table 1: Comparison of relative and absolute changes between cases.

	Age and Sex	Location	Rupture Status	Treatment Performed	Residual Aneurysm Area[a]	Residual Aneurysm Volume[a]	AVG WSS	AVG WSS	Low WSS Area	High WSS Area	Decision CM or RT	Follow-up
Case 1	62 yrs F	MCA Bifurcation	Unruptured	Clip	45.69%%	58.61%	+23.67% (+3.38 Pa)	↑	→	→	CM	7 yrs
Case 2	63 yrs M	PComA-ICA	Unruptured	Coil	18.45%	9.35%	+191.43% (+0.67 Pa)	↑	→	↓	FDS	7 mo
Case 3	69 yrs F	PComA-ICA	Unruptured	Coil	32.31%	32.78%	+137.59% (+1.94 Pa)	↑	→	↓	FDS	7 mo
Case 4	63 yrs F	BA Apex	Unruptured	Coil+Stent	35.17%	12.07%	+200.83% (+4.84 Pa)	↑	↓	↓	YSC	6 mo
Case 5	56 yrs M	MCA Bifurcation	Unruptured	Coil+Stent	11.46%	16.38%	+94.71% (+2.32 Pa)	↑	→	↓	CM	9 yrs
Case 6	61 yrs M	BA Apex	Ruptured	Coil	37.28%	22.37%	-9.96% (-0.83 Pa)	↓	→	↓	CM	3 yrs

AVG, average; BA, basilar artery; CM, conservative management; F, female; FDS, flow diverter stent; M, male; MCA, middle cerebral artery; Mo, months; Pa, Pascal (N/m^2); PComA-ICA, bifurcation of the posterior communicating artery with the internal carotid artery; RT, retreatment; WSS, wall shear stress; Yrs, years; YSC, Y stenting and coils. [a]Percentage relative to pre-treatment total value

increased by 23.67% (+3.38 Pa), the analysis showed a decrease in the low WSS area (0.2–0.006%) and high WSS area (99.1–94.6%).

Illustrative case (PComA)

A 63-year-old male presenting with mental confusion and undergoing investigation for intestinal neoplasia was found to have an aneurysm at the bifurcation of the PComA with the ICA on magnetic resonance imaging (MRI), along with adjacent temporal lobe edema. To protect the aneurysm dome, partial embolization was performed before gastrointestinal oncologic surgery. The protective embolization reduced the aneurysm to 9.35% of its initial volume and showed increased average WSS (+191.43%) and high WSS area (0.5–4.87%), along with decreased low WSS area (74.9–66.7%) in the hemodynamic analysis [Figure 2].

Subsequently, a flow-diverter was deployed, resulting in a complete occlusion of the aneurysm at the latest angiographic follow-up [Figure 3].

Illustrative case (basilar artery apex)

A 63-year-old female was diagnosed with an unruptured aneurysm at the apex of the basilar artery following an MRI scan in a workup for dizziness. Endovascular embolization was performed using coils and a stent (Neuroform Atlas) placed under the P1 segment of the left PCA, originating from the basilar artery. Following this intervention, the aneurysm showed a residual volume of 12.07% of the initial size, accompanied by increases in average WSS (+200.83%); [Figure 4] but also had increased areas of both high WSS (from 6.23 to 33.6%) and low WSS (from 1.38 to 7.82%); [Figure 5].

Given these hemodynamic results indicating an increased risk of rupture, a decision was made for re-intervention by placing an additional stent in the P1 segment of the right PCA to the basilar artery, configuring a Y-stent, along with additional coil embolization [Figure 6]. In the latest follow-up, the aneurysm was completely occluded.

DISCUSSION

Key findings

In this computational flow dynamics analysis, we observed a consistent reduction in both the area (median 33.74%; IQR = 18.83%) and volume (median 19.37%; IQR = 23.43%) across all six residual aneurysms. Furthermore, we noted significant variability in the alteration patterns of average WSS, regions with high and low WSS, and changes in flow velocities within terminal branches. Of note, the prevalent trend among the observed changes was an augmentation in

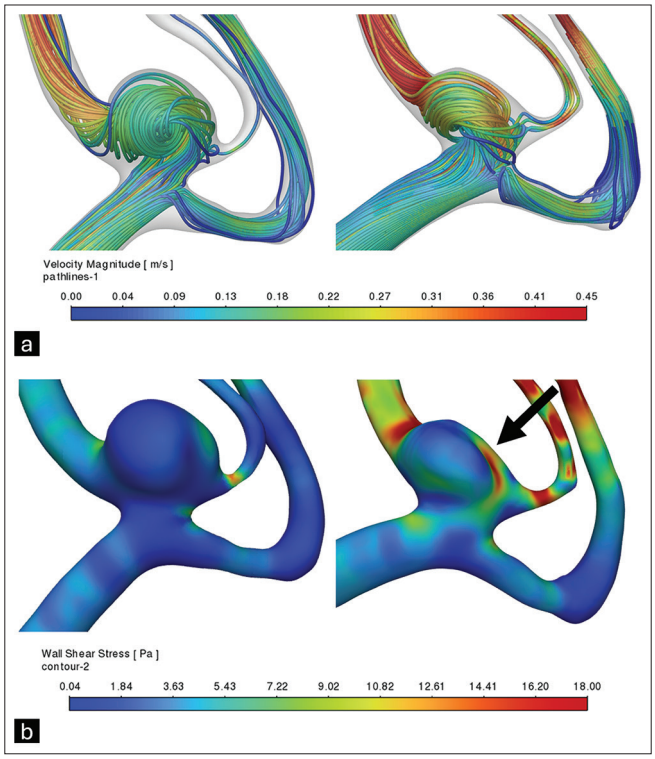

Figure 1: Reconstruction and hemodynamic analysis of the middle cerebral artery bifurcation aneurysm before and after clipping. (a) Estimated blood velocity along the aneurysm and adjacent arteries. (b) Estimated wall shear stress on the aneurysm and adjacent arterial walls, demonstrating elevated wall shear stress adjacent to the surgical clip site (arrow).

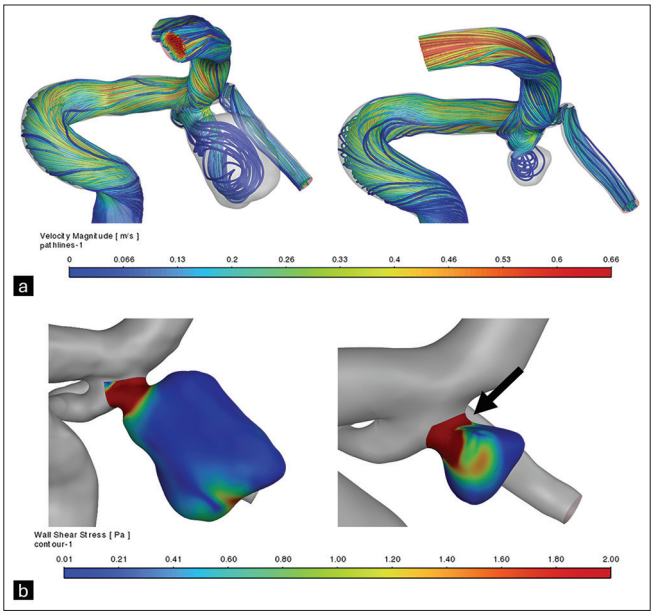

Figure 2: Reconstruction and hemodynamic analysis of the posterior communicating artery-internal carotid artery bifurcation aneurysm before and after coiling. (a) Estimated blood velocity along the aneurysm and adjacent arteries. (b) Estimated wall shear stress on the walls of the aneurysm, demonstrating an increase in wall shear stress near the aneurysm neck region (arrow).

Figure 3: Post-reintervention images of the posterior communicating artery-internal carotid artery bifurcation aneurysm. (a) Left internal carotid artery injection oblique view follow-up showing complete occlusion of the left posterior communicating artery aneurysm post-endovascular treatment. (b) Plain X-ray showing the flow diverter stent and coils placed inside the aneurysm sac.

average WSS (median increase of 137.6%; IQR = 59.2–196.1) coupled with a concurrent decrease in low WSS areas. This trend underscores the potential utility of segmental analysis in assessing surface area variations of aneurysms and understanding the implications of low WSS regions on rupture risk. Among the six cases examined, one exhibited a distinct pattern characterized by an increase in average WSS alongside elevated areas of low WSS. This particular case, we posit, presents the highest likelihood of rupture and warrants closer surveillance.

Interpretation

To gauge the rupture risk post-treatment for aneurysms that had ruptured before initial intervention (i.e., with subarachnoid hemorrhage), a noteworthy study by Johnston *et al.*[7] yielded interesting results. Among 1001 patients followed for an average of 4.0 years, the study revealed a strong association between the degree of aneurysm occlusion post-treatment and the risk of rupture. The overall risk varied from 1.1% for complete occlusion, 2.9% for 91–99% occlusion, 5.9% for 70–90% occlusion, and 17.6% for <70% occlusion ($P < 0.0001$). This adds a crucial factor to be considered in the risk stratification for rupture of residual aneurysms, indicating that those with a larger residual portion would benefit even more from reinterventions, given their progressively higher risk of rupture with increasing residual size.

Out of our six studied cases, only one of the aneurysms was ruptured at the initial presentation. Past cohorts have evaluated the risk of rupture for residual aneurysms according to the aneurysm rupture status, especially in cases treated

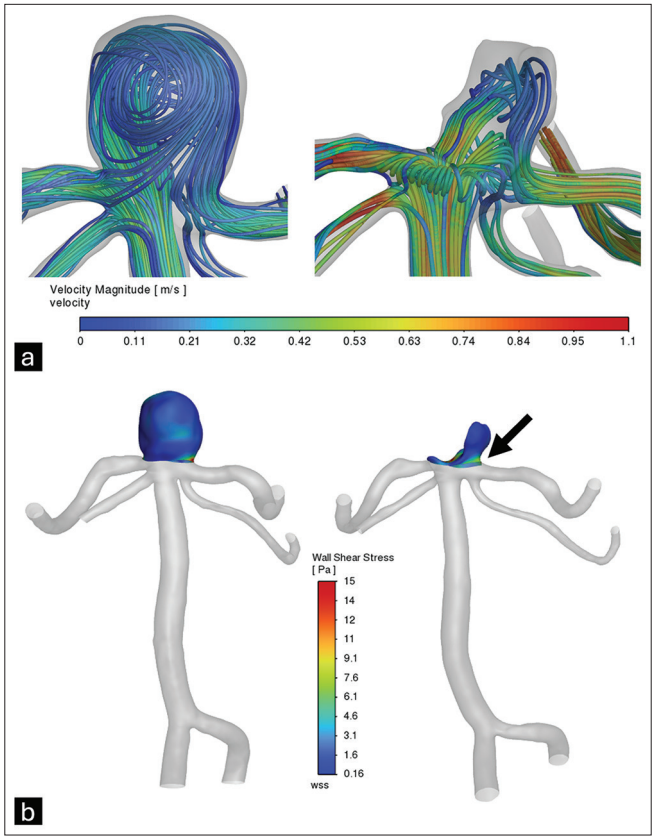

Figure 4: Reconstruction and hemodynamic analysis of the basilar artery apex aneurysm before and after single stent (from left P1 to basilar artery). (a) Velocity streamlines indicate inflow predilection to the right side of the aneurysm wall before treatment and interruption of the main streamlines due to coils after coil embolization. (b) Reduction in aneurysm volume after coil embolization, with residual aneurysm showing increased wall shear stress, partially visualized in this incidence near the neck (arrow).

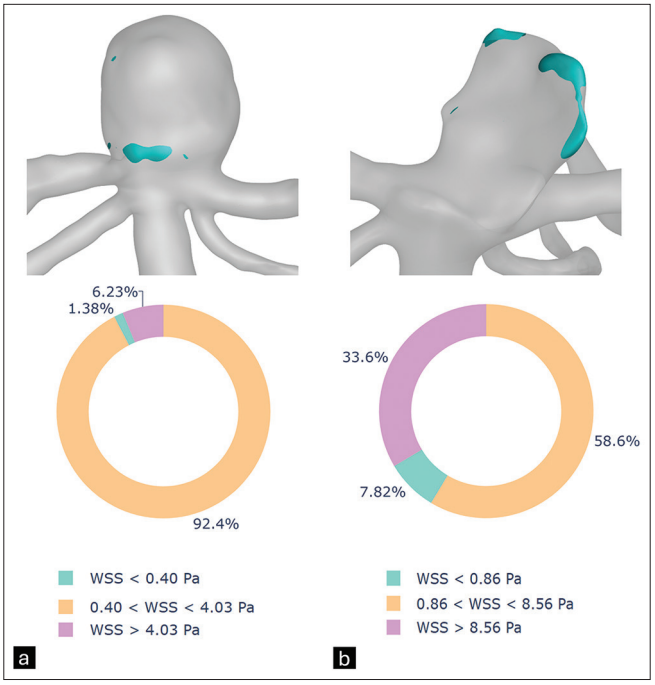

Figure 5: Hemodynamic analysis of the surface of the basilar artery apex aneurysm, demonstrating increase in the low wall shear stress area compared to before treatment. (a) Before initial treatment. (b) After initial treatment.

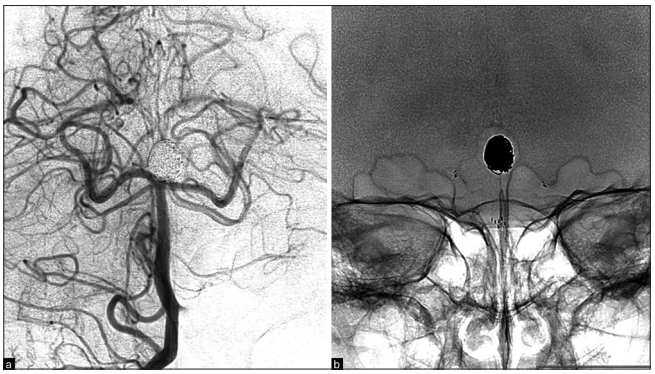

Figure 6: Post-reintervention images of the basilar artery apex aneurysm, demonstrating complete occlusion after retreatment with additional stent (Y-stenting) and coils. (a) Basilar digital subtraction angiography with right vertebral artery selective angiography. (b) Plain X-ray showing the Y-stenting and coils.

with coils. In an insightful study by Munich *et al.*,[9] among 626 aneurysms exhibiting residual filling immediately post-treatment, 13 (2.1%) ruptured during the follow-up period (mean 7.3 months; range 1–84 months), most of whom were ruptured aneurysms at initial presentation (84.6%). This indicates a low rupture risk for unruptured aneurysms with residual necks (0.6%) but a significantly higher risk of re-rupture for ruptured aneurysms treated in the acute setting (3.4%). This underscores the importance of prior rupture status in stratifying rupture risk for these cases of residual aneurysms. The findings indicating higher rupture risk for previously ruptured cases, along with the progressively increased risk of rupture with a greater residual portion of these aneurysms, underscore the importance of studying and closely monitoring these previously ruptured cases with larger residual portions post-treatment. Particularly, these cases may benefit from further investigation, such as through CFD analysis.

In our results, the decreasing trend of the low WSS areas in most cases (five of the six cases) could indicate a reduction in regions prone to thrombus formation[2,13] and be associated with a lower risk of rupture.[22] This decrease in low WSS areas may stem from coil embolization obliterating thrombus-prone areas or clipping obliterating these regions. On the other hand, the observed increase in average WSS and the corresponding decrease in low WSS areas in four of the six cases post-

Table 2: Percentage changes in the areas of each wall shear stress category before and after intervention, classified by low, intermediate, and high wall shear stress.

	Low WSS are[a]			Intermediate WSS are[a]			High WSS are[a]		
	Before[a]	After[a]	Difference[b]	Before[a]	After[a]	Difference[b]	Before[a]	After[a]	Difference[b]
Case 1	0.2%	0.06%	-70%	0.7%	5.31%	658.6%	99.1%	94.6%	-4.54%
Case 2	74.9%	66.7%	-10.95%	24.6%	28.4%	15.45%	0.5%	4.87%	874%
Case 3	55.8%	4.98%	-91.08%	39%	85.9%	120.26%	5.2%	9.11%	75.19%
Case 4	1.38%	7.82%	466.67%	92.4%	58.6%	-36.58%	6.23%	33.6%	439.33%
Case 5	7.49%	3.57%	-52.34%	84.2%	61.9%	-26.48%	8.28%	34.6%	317.87%
Case 6	21.7%	6.15%	-71.66%	29.1%	43.2%	48.45%	49.2%	50.6%	2.85%

WSS, wall shear stress. [a]Percentage of the total surface area of the aneurysm subjected to low, intermediate, or high wall shear stress. [b]Percentage change in the distributions of areas:

intervention could suggest a complex interaction between stability and rupture risk factors. High WSS has been associated with aneurysm growth and rupture due to the mechanical stress it exerts on the aneurysm wall, potentially leading to structural changes.[4,15,22] Conversely, low WSS has been linked to the growth phase and rupture of cerebral aneurysms by causing degenerative changes in the aneurysm wall.[15]

Notably, the only case with an increase in low WSS area was the one with the highest increase in average WSS, both in relative (+200.83%) and absolute terms (+4.84 Pa). This case, with an increase in low WSS area and the highest increase in WSS, may represent a higher-risk scenario due to the potential for residual thrombus formation and greater mechanical stress on the aneurysm wall, which could lead to instability and necessitate closer monitoring.[4,15,22]

This result underscores the intricate relationship between hemodynamic parameters and the risk of cerebral aneurysm rupture or stability post-intervention. While the pre-treatment unruptured state and significant reductions in aneurysm size imply a lower risk of rupture, the interplay between increased WSS and increased low WSS area highlights the need for careful post-treatment monitoring to avoid complications.

Limitations and generalizability

Our study, although informative, has several limitations that must be considered. First, the retrospective design and small sample size of six patients may limit the generalizability of our findings. In addition, the use of CFD introduces inherent assumptions and simplifications that could affect the accuracy of our results. Furthermore, while we focused on key hemodynamic parameters such as WSS and low WSS area, other factors influencing treatment outcomes were not explored. Finally, interpreting hemodynamic changes post-intervention requires consideration of various clinical and imaging factors. Thus, while our study provides valuable insights, further research with larger samples and comprehensive approaches is warranted to validate and extend our findings.

CONCLUSION

Residual IAs display diverse hemodynamic responses following clipping or coiling procedures. The observed increase in high WSS area and average WSS, coupled with a decrease in low WSS area, suggests a complex interaction between stability and rupture risk factors. Conversely, an increase of all parameters may indicate the riskiest scenario due to greater mechanical stress on the aneurysm wall, potentially leading to instability and rupture and requiring closer monitoring.

Ethical approval

The research/study is approved by the Institutional Review Board at Hospital Israelita Albert Einstein, number 6.713.150, dated March 20, 2024.

Declaration of patient consent

The authors certify that they have obtained all appropriate patient consent.

Financial support and sponsorship

Nil.

Conflicts of interest

There are no conflicts of interest.

Use of artificial intelligence (AI)-assisted technology for manuscript preparation

The authors confirm that there was no use of artificial intelligence (AI)-assisted technology for assisting in the writing or editing of the manuscript and no images were manipulated using AI.

REFERENCES

1. Aguiar GB, Kormanski MK, Corrêa CJ, Batista AV, Conti ML, Veiga JC. Residual lesions in patients undergoing microsurgical clipping of cerebral aneurysms in a reference university hospital. Clinics 2020;75:e1973.
2. Bass DI, Marsh LM, Fillingham P, Lim D, Chivukula VK, Kim LJ, *et al*. Modeling the mechanical microenvironment of coiled cerebral aneurysms. J Biomech Eng 2023;145:041005.
3. Bederson JB, Awad IA, Wiebers DO, Piepgras D, Haley EC, Brott T, *et al*. Recommendations for the management of patients with unruptured intracranial aneurysms. Circulation 2000;102:2300-8.
4. Dolan JM, Kolega J, Meng H. High wall shear stress and spatial gradients in vascular pathology: A review. Ann Biomed Eng 2013;41:1411-27.
5. Ford MD, Alperin N, Lee SH, Holdsworth DW, Steinman DA. Characterization of volumetric flow rate waveforms in the normal internal carotid and vertebral arteries. Physiol Meas 2005;26:477-88.
6. Hu S, Chen R, Xu W, Li H, Yu J. A predictive hemodynamic model based on risk factors for ruptured mirror aneurysms. Front Neurol 2022;13:998557.
7. Johnston SC, Dowd CF, Higashida RT, Lawton MT, Duckwiler GR, Gress DR. Predictors of rehemorrhage after treatment of ruptured intracranial aneurysms. Stroke 2008;39:120-5.
8. Jou LD, Lee DH, Morsi H, Mawad ME. Wall shear stress on ruptured and unruptured intracranial aneurysms at the internal carotid artery. Am J Neuroradiol 2008;29:1761-7.
9. Munich SA, Cress MC, Rangel-Castilla L, Sonig A, Ogilvy CS, Lanzino G, *et al*. Neck remnants and the risk of aneurysm rupture after endovascular treatment with coiling or stent-assisted coiling: Much ado about nothing? Neurosurgery 2019;84:421-7.
10. Murias Quintana E, Gil Garcia A, Vega Valdés P, Cuellar H, Meilán Martínez Á, Saiz Ayala A, *et al*. Anatomical results, rebleeding and factors that affect the degree of occlusion in ruptured cerebral aneurysms after endovascular therapy. J Neurointerv Surg 2015;7:892-7.
11. Obermueller K, Hostettler I, Wagner A, Boeckh-Behrens T, Zimmer C, Gempt J, *et al*. Frequency and risk factors for postoperative aneurysm residual after microsurgical clipping. Acta Neurochir (Wien) 2021;163:131-8.
12. Qiu T, Jin G, Xing H, Lu H. Association between hemodynamics, morphology, and rupture risk of intracranial aneurysms: A computational fluid modeling study. Neurol Sci 2017;38:1009-18.
13. Rayz VL, Boussel L, Lawton MT, Acevedo-Bolton G, Ge L, Young WL, *et al*. Numerical modeling of the flow in intracranial aneurysms: Prediction of regions prone to thrombus formation. Ann Biomed Eng 2008;36:1793-804.
14. Sauvigny J, Drexler R, Pantel TF, Ricklefs FL, Catapano JS, Wanebo JE, *et al*. Microsurgical clipping of unruptured anterior circulation aneurysms-a global multicenter investigation of perioperative outcomes. Neurosurgery 2024;94:1218-26.
15. Shojima M, Oshima M, Takagi K, Torii R, Hayakawa M, Katada K, *et al*. Magnitude and role of wall shear stress on cerebral aneurysm. Stroke 2004;35:2500-5.
16. Spiessberger A, Vogt DR, Fandino J, Marbacher S. Formation of intracranial *de novo* aneurysms and recurrence after neck clipping: A systematic review and meta-analysis. J Neurosurg 2020;132:456-64.
17. Tian Z, Li X, Wang C, Feng X, Sun K, Tu Y, *et al*. Association between aneurysmal hemodynamics and rupture risk of unruptured intracranial aneurysms. Front Neurol 2022;13:818335.
18. Tsutsumi K, Ueki K, Usui M, Kwak S, Kirino T. Risk of recurrent subarachnoid hemorrhage after complete obliteration of cerebral aneurysms. Stroke 1998;29:2511-3.
19. Wang JW, Li CH, Liu JF, Li H, Guo H, Gao BL. Endovascular treatment of multiple intracranial aneurysms. Medicine 2023;102:e36340.
20. Wermer MJ, Rinkel GJ, Greebe P, Albrecht KW, Dirven CM, Tulleken CA. Late recurrence of subarachnoid hemorrhage after treatment for ruptured aneurysms: Patient characteristics and outcomes. Neurosurgery 2005;56:197-204.
21. Zarrinkoob L, Ambarki K, Wåhlin A, Birgander R, Eklund A, Malm J. Blood flow distribution in cerebral arteries. J Cereb Blood Flow Metab 2015;35:648-54.
22. Zhou G, Zhu Y, Yin Y, Su M, Li M. Association of wall shear stress with intracranial aneurysm rupture: Systematic review and meta-analysis. Sci Rep 2017;7:5331.

How to cite this article: Ogilvy CS, Tatit RT, Loly VT, Ramirez-Velandia F, Lima JS ,Baccin CE *et al*. Exploring the hemodynamic behavior of residual aneurysms after coiling and clipping: A computational flow dynamic analysis. Surg Neurol Int. 2024;15:376. doi: 10.25259/SNI_686_2024